AIAA JOURNAL
Vol. 31, No. 6, June 1993

Interlaminar Stresses Around a Hole in Symmetric Cross-Ply Laminates Under Bending/Torsion

Chu-Cheng Ko* and Chien-Chang Lin†
National Chung-Hsing University, Taichung, Taiwan 40227, Republic of China

An efficient approximate solution for calculating the complete state of stress around a circular hole in symmetric cross-ply laminates under a set of far-field bending and torsion is presented. This approach is based on the boundary-layer theory in conjunction with Lekhnitskii's solutions for anisotropic plates and the principle of minimum complementary energy. All of the boundary conditions around the hole edge of each ply and traction continuity at the ply interface are exactly satisfied. Numerical examples are compared with the NASTRAN finite element solutions to demonstrate the efficiency and accuracy of the current method.

I. Introduction

THE importance of the free-edge effect in the strength determination of composite laminates is widely recognized. Because of the stiffness discontinuity between plies, it is well known that the interlaminar stresses exist around the free edge region; moreover, these interlaminar stresses may induce delamination failure near the hole boundary, especially under fatigue loading. It is also well known that classical lamination theory, using the hypothesis of plane stress, is incapable of providing prediction of such phenomena; therefore, a correct prediction for the interlaminar stress components near the free edge is required.

Since 1970, numerous research works[1-6] have developed a variety of analyses to determine the interlaminar stresses at the straight free edge of composite laminates under in-plane, bending, and torsional loads. Pipes and Pagano[1] used the anisotropic elasticity theory in conjunction with the finite difference method to analyze a simple four-ply laminate subjected to uniform axial tension. Salamon[2] extended Pipes and Pagano's finite difference method for laminates with applied pure bending. Wang and Crossman[3] proposed a quasi-three-dimensional finite element model to obtain the interlaminar stresses under tension. Chan and Ochoa[4] developed a finite element model for the edge delamination analysis of composite laminates subjected to tension, bending, and torsional loads. Wang and Choi[5] derived an analytical solution by using Lekhnitskii's stress potentials and the theory of anisotropic elasticity to determine the stress singularity order at the free edges of a laminate under tension. Kassapoglou and Lagace[6] developed an efficient technique to analyze the interlaminar stress distributions under tension by the assumption of stress shapes and the use of the principle of minimum complementary energy.

The analysis of the free-edge effect becomes much more difficult for curved edges due to the complicated geometry and inherent three-dimensional stress variations. A boundary-layer theory developed by Reiss[7] has been extended to composite laminates by Tang[8] by separating this problem into two equivalent problems, namely, a modified torsion problem and a modified plane strain problem. Zhang and Ueng[9] proposed a simplified method to investigate the effect of the ratio of hole radius to laminate thickness on the interlaminar stress distributions around a hole in a $(0/90\ \text{deg})_s$ laminate under far-field tensile or shear stress. Several studies[10-13] employed three-dimensional finite element methods for calculating the interlaminar stresses around the hole of composite laminates. The results of these studies are based on the conventional displacement formulations so that compatibility is exactly satisfied whereas the equilibrium equations and traction-free-edge boundary conditions are only approximately satisfied. This drawback may lead to questionable stress results near the free edge, which has been emphasized by Spilker and Chou.[14] In addition, one of the shortcomings of the finite element methods is that they may be very inefficient for laminates with numerous plies. In an effort to develop an efficient method, the authors[15] used the boundary-layer theory in conjunction with the assumed stress functions and the principle of minimum complementary energy to obtain the interlaminar stresses around the hole region due to in-plane loads. However, all aforementioned investigations for laminates with curved free edges considered in-plane loads only. Bradshaw and Pang[16] used the classical lamination plate theory in conjunction with point stress, average stress failure hypothesis, and Tsai-Wu failure criterion to determine the failure loads for laminates with circular holes under bending. However, no free edge effect has been considered in Ref. 16. No literature, to the best of the authors' knowledge, has been found for laminates with curved free edges under bending or torsional load.

The purpose of this investigation is to develop an efficient method for estimating the three-dimensional stresses around a circular hole in symmetric cross-ply laminates under a set of far-field pure bending and torsional loads. Here, the authors' recently proposed efficient method[15] for calculating the interlaminar stresses around a circular hole under in-plane loads is extended, and Lekhnitskii's solutions for anisotropic plates[17] are used. Numerical results obtained from the present method are compared with the NASTRAN[18] finite element solutions to demonstrate the efficiency and accuracy of this method.

II. Method of Stress Analysis

Consider a symmetric cross-ply laminate that consists of N plies of equal thickness t and a circular hole of radius R subjected to a set of bending and torsional loads at infinity as shown in Fig. 1.

The equilibrium equations for the kth ply, in the absence of body forces, have the following form:

$$\begin{aligned}
&\frac{\partial \sigma_{rr}^{(k)}}{\partial r}+\frac{1}{r}\frac{\partial \tau_{r\theta}^{(k)}}{\partial \theta}+\frac{\partial \tau_{rz}^{(k)}}{\partial z}+\frac{\sigma_{rr}^{(k)}-\sigma_{\theta\theta}^{(k)}}{r}=0\\
&\frac{\partial \tau_{r\theta}^{(k)}}{\partial r}+\frac{1}{r}\frac{\partial \sigma_{\theta\theta}^{(k)}}{\partial \theta}+\frac{\partial \tau_{z\theta}^{(k)}}{\partial z}+\frac{2\tau_{r\theta}^{(k)}}{r}=0 \qquad (1)\\
&\frac{\partial \tau_{rz}^{(k)}}{\partial r}+\frac{1}{r}\frac{\partial \tau_{z\theta}^{(k)}}{\partial \theta}+\frac{\partial \sigma_{zz}^{(k)}}{\partial z}+\frac{\tau_{rz}^{(k)}}{r}=0
\end{aligned}$$

Received Jan. 15, 1992; revision received Sept. 15, 1992; accepted for publication Sept. 17, 1992.

*Graduate Student, Institute of Applied Mathematics.
†Professor, Institute of Applied Mathematics. Member AIAA.

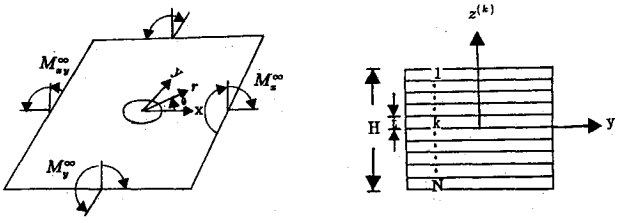

Fig. 1 Laminate geometry and loadings.

where $\sigma_{rr}^{(k)}$, $\sigma_{\theta\theta}^{(k)}$, and $\sigma_{zz}^{(k)}$ are normal stress components, and $\tau_{r\theta}^{(k)}$, $\tau_{rz}^{(k)}$, and $\tau_{z\theta}^{(k)}$ are shear stress components of the kth ply in terms of polar coordinates.

Analogous to Refs. 7 and 8, nondimensional variables are introduced as follows:

$$\xi = (r - R)/R, \qquad \xi \geq 0; \qquad \rho = z^{(k)}/t, \quad 0 \leq \rho \leq 1$$

$$\epsilon = t/R; \qquad \eta = \xi/\epsilon$$

The equilibrium equations for the kth ply have the same form as those in Refs. 7 and 8:

$$\begin{aligned}
&\tau_{rz,\rho}^{(k)} + \epsilon\left\{\sigma_{rr,\xi}^{(k)} + \frac{1}{1+\xi}\left[\tau_{r\theta,\theta}^{(k)} + \sigma_{rr}^{(k)} - \sigma_{\theta\theta}^{(k)}\right]\right\} = 0 \\
&\tau_{z\theta,\rho}^{(k)} + \epsilon\left\{\tau_{r\theta,\xi}^{(k)} + \frac{1}{1+\xi}\left[\sigma_{\theta\theta,\theta}^{(k)} + 2\tau_{r\theta}^{(k)}\right]\right\} = 0 \qquad (2) \\
&\sigma_{zz,\rho}^{(k)} + \epsilon\left\{\tau_{rz,\xi}^{(k)} + \frac{1}{1+\xi}\left[\tau_{z\theta,\theta}^{(k)} + \tau_{rz}^{(k)}\right]\right\} = 0
\end{aligned}$$

Now the solution procedures presented by the present authors[15] for considering in-plane loads are followed in this study. The whole region consists of the interior and boundary-layer region, and each stress component is obtained by combining the interior stress σ_{ij}^0, and boundary-layer stress f_{ij}. In the interior region, Lekhnitskii's solutions for anisotropic plates[17] together with classical lamination plate theory[19] are employed. In the vicinity of the free edge around the hole, namely, the boundary-layer region, a three-dimensional stress analysis of each ply is essential. A boundary-layer theory based on the perturbation technique developed by Reiss[7] and extended by Tang[8] is used. Stress functions for each ply are assumed according to the zeroth-order boundary-layer equilibrium equations, and then the boundary-layer stress is obtained as a complementary term superimposed on the interior stress so that the boundary conditions for each ply and traction continuity at ply interface are exactly satisfied. With this idealization, it is possible to obtain the free-edge stress solutions of this problem.

The equilibrium equations in the boundary-layer region are approximated by the perturbation expansions of the boundary-layer stress components f_{ij} in terms of the single parameter ϵ as follows:

$$f_{ij}(\eta, \theta, \rho, \epsilon) = \sum_{n=0}^{\infty} f_{ij}^{(n)}(\eta, \theta, \rho)\epsilon^n \qquad (3)$$

where $f_{ij}^{(n)} = 0$ for $n < 0$, and $i, j = r, \theta, z$.

Substituting Eqs. (3) into Eqs. (2) and equating the coefficients of the like powers of ϵ lead to a series of differential equations for the boundary layer. In the zeroth-order approximation, the terms in the zeroth power of ϵ are equated, and the following equilibrium equations can be obtained:

$$\begin{aligned}
&f_{rz,\rho}^{0(k)} + f_{rr,\eta}^{0(k)} = 0 \\
&f_{z\theta,\rho}^{0(k)} + f_{r\theta,\eta}^{0(k)} = 0 \qquad (4) \\
&f_{zz,\rho}^{0(k)} + f_{rz,\eta}^{0(k)} = 0
\end{aligned}$$

The higher order approximations can be obtained in a similar manner.

A. Stress Solutions for Interior Region

From classical lamination plate theory, the moment resultant-curvature relations for a symmetric laminate can be written in the following matrix form:

$$\begin{Bmatrix} M_x \\ M_y \\ M_{xy} \end{Bmatrix} = \begin{bmatrix} D_{11} & D_{12} & D_{16} \\ D_{12} & D_{22} & D_{26} \\ D_{16} & D_{26} & D_{66} \end{bmatrix} \begin{Bmatrix} \kappa_x \\ \kappa_y \\ \kappa_{xy} \end{Bmatrix} \qquad (5)$$

where the D_{ij} are the bending stiffnesses of the laminate.[19]

In this study, laminates with symmetric and cross-ply construction (i.e., $D_{16} = D_{26} = 0$) are considered. According to Lekhnitskii's solutions[17] for an orthotropic plate, the moment resultant expressions at the edge of the hole, under a set of far-field bending and torsional loads M_x^{∞}, M_y^{∞}, and M_{xy}^{∞}, are given as follows:

$$\begin{aligned}
M_\theta = {} & M_x^{\infty}\left[1 + \frac{\sqrt{D_{11}D_{22}}}{D_{rr}}\frac{1}{(k+4g)}(b_0\sin^4\theta\right. \\
& \left. + b_2\sin^2\theta\cos^2\theta + b_4\cos^4\theta)\right] \\
& + M_y^{\infty}\left[1 + \frac{\sqrt{D_{11}D_{22}}}{D_{rr}}\frac{1}{(k+4g)}(c_0\sin^4\theta\right. \\
& \left. + c_2\sin^2\theta\cos^2\theta + c_4\cos^4\theta)\right] \\
& - 2M_{xy}^{\infty}\frac{\sqrt{D_{11}D_{22}}}{D_{rr}}\frac{n(k+n+1)}{n(k+1)+2(\nu_{xy}+k)}\sin\theta\cos\theta \\
& \times\left[\frac{1+\nu_{xy}}{k}\sin^2\theta + (1+\nu_{yx})k\cos^2\theta\right] \qquad (6a)
\end{aligned}$$

$$\begin{aligned}
M_{r\theta} = {} & M_x^{\infty}\frac{\sqrt{D_{11}D_{22}}}{D_{rr}}\frac{1}{(k+4g)}(b_1\sin^2\theta + b_3\cos^2\theta)\sin\theta\cos\theta \\
& + M_y^{\infty}\frac{\sqrt{D_{11}D_{22}}}{D_{rr}}\frac{1}{(k+4g)}(c_1\sin^2\theta + c_3\cos^2\theta)\sin\theta\cos\theta \\
& + M_{xy}^{\infty}\frac{\sqrt{D_{11}D_{22}}}{D_{rr}}\frac{n(k+n+1)}{n(k+1)+2(\nu_{xy}+k)}\left(k\cos^4\theta - \frac{1}{k}\sin^4\theta\right) \qquad (6b)
\end{aligned}$$

where

$$k = \sqrt{\frac{D_{11}}{D_{22}}}, \qquad g = \frac{D_{66}}{D_{22}(1-\nu_{xy}\nu_{yx})}, \qquad n = -i(\mu_1 + \mu_2)$$

$$D_{rr} = D_{11}\cos^4\theta + 2(D_{12} + 2D_{66})\sin^2\theta\cos^2\theta + D_{22}\sin^4\theta$$

$$b_0 = n$$

$$b_1 = -n - 1 + 2g\left(\nu_{yx} + \nu_{yx}n - \frac{1}{k}\right)$$

$$b_3 = k - n - n^2 - 1 + 4g(1+\nu_{yx})(1+n)$$

$$b_4 = k[1 - k - 4g(1+\nu_{yx})$$

$$c_0 = k - 1 - 4g\frac{1+\nu_{xy}}{k}$$

$$c_1 = -k + 2g\left(\frac{n+n^2}{k} + \nu_{yx}k - 1\right)$$

$$c_2 = k(1-k-n) - n^2 + 4g(1-\nu_{xy})\left(\frac{n}{k} + 1\right)$$

$$c_3 = k(k+n) + 2g\left(k - \nu_{xy} - \frac{\nu_{xy}n}{k}\right)$$

$$c_4 = kn$$

$$\nu_{xy} = \frac{D_{12}}{D_{22}}$$

$$\nu_{yx} = \frac{D_{12}}{D_{11}}$$

and where $i = \sqrt{-1}$, and μ_1 and μ_2 are the complex roots obtained from the following characteristic equation[17]:

$$D_{22}\mu^4 + 2(D_{12} + 2D_{66})\mu^2 + D_{11} = 0 \tag{7}$$

Using the classical lamination plate theory and transformation of coordinates, the in-plane stress components around the edge of the hole can be written as

$$\begin{Bmatrix} \sigma^0_{rr} \\ \sigma^0_{\theta\theta} \\ \tau^0_{r\theta} \end{Bmatrix}^{(k)}_{\eta=0} = \begin{Bmatrix} a_1 \\ a_2 \\ a_3 \end{Bmatrix}^{(k)} [t_0^{(k)} + \rho^{(k)}t] \tag{8}$$

where $t_0^{(k)}$ is the distance from the midplane to the bottom of the kth ply, and

$$\begin{Bmatrix} a_1 \\ a_2 \\ a_3 \end{Bmatrix}^{(k)} = [T][\bar{Q}]^{(k)}[D]^{-1}[T]^{-1} \begin{Bmatrix} 0 \\ M_\theta \\ M_{r\theta} \end{Bmatrix}_{\eta=0}$$

where

$[T]$ = coordinate transformation matrix
$[\bar{Q}]^{(k)}$ = transformed stiffness matrix of the kth ply in xy coordinates
$[D]$ = laminate bending stiffness matrix

B. Stress Solutions for Boundary-Layer Region

According to the equilibrium equations of the zeroth-order approximation, the stress solutions can be developed for the kth ply by assuming that each stress component, except for $f^{0(k)}_{\theta\theta}$, can be expressed as the product of two independent functions:

$$f^{0(k)}_{ij} = g^{(k)}_{ij}(\rho)h^{(k)}_{ij}(\eta) \tag{9}$$

where $g^{(k)}_{ij}(\rho)$ and $h^{(k)}_{ij}(\eta)$ are unknown functions for each ply in the laminate.

Substituting Eqs. (9) into the zeroth-order approximate equations, Eqs. (4) yields the following equations for the unknown functions:

$$\frac{dg^{(k)}_{rz}}{d\rho} = g^{(k)}_{rr} \tag{10a}$$

$$\frac{dg^{(k)}_{zz}}{d\rho} = g^{(k)}_{rz} \tag{10b}$$

$$\frac{dg^{(k)}_{z\theta}}{d\rho} = g^{(k)}_{r\theta} \tag{10c}$$

$$-\frac{dh^{(k)}_{rr}}{d\eta} = h^{(k)}_{rz} \tag{11a}$$

$$-\frac{dh^{(k)}_{rz}}{d\eta} = h^{(k)}_{zz} \tag{11b}$$

$$-\frac{dh^{(k)}_{r\theta}}{d\eta} = h^{(k)}_{z\theta} \tag{11c}$$

It can be observed that the required minimum number of the unknown functions $g^{(k)}_{ij}(\rho)$ and $h^{(k)}_{ij}(\eta)$ is four in each ply and the remaining functions can be obtained by using Eqs. (10a–10c) and (11a–11c) on the condition that boundary conditions and traction continuity are satisfied.

In view of Eqs. (10a–10c), $g^{(k)}_{rr}$ and $g^{(k)}_{r\theta}$ are selected as the basic approximate functions. In general, the classical lamination plate theory predicts that in-plane stresses are at most linear in the thickness direction of each ply. Therefore, the in-plane stress components $g^{(k)}_{rr}$ and $g^{(k)}_{r\theta}$ for the boundary-layer region are assumed to be linear functions of P:

$$g^{(k)}_{rr} = B^{(k)}_2 + B^{(k)}_1\rho \tag{12a}$$

$$g^{(k)}_{r\theta} = B^{(k)}_6 + B^{(k)}_5\rho \tag{12b}$$

Substituting Eqs. (12a) and (12b) into Eqs. (10a–10c) yields the remaining functions for $g^{(k)}_{ij}(\rho)$ in the kth ply:

$$g^{(k)}_{rz} = \tfrac{1}{2}B^{(k)}_1\rho^2 + B^{(k)}_2\rho + B^{(k)}_3 \tag{12c}$$

$$g^{(k)}_{zz} = \tfrac{1}{6}B^{(k)}_1\rho^3 + \tfrac{1}{2}B^{(k)}_2\rho^2 + B^{(k)}_3\rho + B^{(k)}_4 \tag{12d}$$

$$g^{(k)}_{z\theta} = \tfrac{1}{2}B^{(k)}_5\rho^2 + B^{(k)}_6\rho + B^{(k)}_7 \tag{12e}$$

Similarly, $h^{(k)}_{rr}$ and $h^{(k)}_{r\theta}$ are selected as our basic approximate functions of η. Because interlaminar stress concentration occurs around the free edge and decays rapidly to zero away from the free edge, $h^{(k)}_{rr}$ and $h^{(k)}_{r\theta}$ are assumed to be exponential functions of η:

$$h^{(k)}_{rr} = A^{(k)}_1\exp(-\lambda_1\eta) + A^{(k)}_2\exp(-\lambda_1\lambda_2\eta) \tag{13a}$$

$$h^{(k)}_{r\theta} = A^{(k)}_3\exp(-\lambda_1\eta) \tag{13b}$$

Substituting Eqs. (13a) and (13b) into Eqs. (11a–11c) yields the remaining functions for $h^{(k)}_{ij}(\eta)$ in the kth ply:

$$h^{(k)}_{rz} = A^{(k)}_1\lambda_1\exp(-\lambda_1\eta) + A^{(k)}_2\lambda_1\lambda_2\exp(-\lambda_1\lambda_2\eta) \tag{13c}$$

$$h^{(k)}_{zz} = A^{(k)}_1\lambda_1^2\exp(-\lambda_1\eta) + A^{(k)}_2\lambda_1^2\lambda_2^2\exp(-\lambda_1\lambda_2\eta) \tag{13d}$$

$$h^{(k)}_{z\theta} = A^{(k)}_3\lambda_1\exp(-\lambda_1\eta) \tag{13e}$$

In the preceding stress expressions, the coefficients $A^{(k)}_i$ and $B^{(k)}_i$ are to be determined by the associated boundary conditions and interface traction continuity.

C. Boundary Conditions and Interface Traction Continuity

The boundary conditions and interface traction continuity of this problem can be given as follows:

1) At infinity, boundary-layer stress components $f^{0(k)}_{ij}$ will vanish and boundary conditions will be satisfied by the interior region in a stress resultant concept:

$$\lim_{\eta\to\infty}\{f^{0(k)}_{rr}, f^{0(k)}_{r\theta}, f^{0(k)}_{rz}, f^{0(k)}_{z\theta}, f^{0(k)}_{zz}\} = 0, \quad k = 1, 2, \ldots, N \tag{14a}$$

2) On the top and bottom surface of the laminate

$$f^{0(k)}_{rz} = f^{0(k)}_{z\theta} = f^{0(k)}_{zz} = 0 \tag{14b}$$

3) At the interface of two adjacent plies

$$f^{0(k)}_{rz} = f^{0(k+1)}_{rz}$$

$$f^{0(k)}_{z\theta} = f^{0(k+1)}_{z\theta}, \qquad k = 1, 2, \ldots, N-1 \tag{14c}$$

$$f^{0(k)}_{zz} = f^{0(k+1)}_{zz}$$

4) Along the hole boundary, i.e., $\eta = 0$,

$$\sigma^{(k)}_{rr} = f^{0(k)}_{rr} + \sigma^{0(k)}_{rr} = 0$$

$$\tau^{(k)}_{r\theta} = f^{0(k)}_{r\theta} + \tau^{0(k)}_{r\theta} = 0 \tag{14d}$$

$$f^{0(k)}_{rz} = 0, \qquad k = 1, 2, \ldots, N$$

D. Stress Solutions for Boundary-Layer Region

Using the assumed stress functions, Eqs. (12a–13e), and the associated boundary conditions, Eqs. (14a) and (14d), coefficients $A_i^{(k)}$ can be given

$$A_1^{(k)} = -A_2^{(k)}\lambda_2 = -\frac{\lambda_2}{\lambda_2 - 1}\, a_1^{(k)} t_0^{(k)}$$

$$A_2^{(k)} = \frac{a_1^{(k)}}{\lambda_2 - 1}\, t_0^{(k)} \tag{15}$$

$$A_3^{(k)} = -a_3^{(k)} t_0^{(k)}$$

Next, from the traction continuity conditions at ply interface, Eqs. (14c), and traction-free conditions at the top and bottom surface of the laminate, Eqs. (14b), coefficients $B_i^{(k)}$ can be obtained:

$$B_1^{(k)} = \frac{t}{t_0^{(k)}}$$

$$B_2^{(k)} = 1$$

$$B_3^{(k)} = \frac{1}{a_1^{(k)} t_0^{(k)}} \left\{ \sum_{j=k+1}^{N} [\tfrac{1}{2}t + t_0^{(j)}] a_1^{(j)} \right\}$$

$$B_4^{(k)} = \frac{1}{a_1^{(k)} t_0^{(k)}} \left\{ \sum_{j=k+1}^{N} [\tfrac{1}{6} a_1^{(j)} t + \tfrac{1}{2} a_1^{(j)} t_0^{(j)}] + \sum_{m=j+1}^{N} [\tfrac{1}{2}t + t_0^{(m)}] a_1^{(m)} \right\} \tag{16}$$

$$B_5^{(k)} = \frac{t}{t_0^{(k)}}$$

$$B_6^{(k)} = 1$$

$$B_7^{(k)} = \frac{1}{a_3^{(k)} t_0^{(k)}} \left\{ \sum_{j=k+1}^{N} [\tfrac{1}{2}t + t_0^{(j)}] a_3^{(j)} \right\}$$

Furthermore, from the interface traction continuity condition, we can conclude that λ_1 and λ_2 are constant through the laminate.

The final stress solutions for the kth ply in the boundary-layer region can be obtained as follows:

$$f_{rr}^{0(k)} = [1 + B_1^{(k)}\rho] A_2^{(k)} [\exp(-\lambda_1\lambda_2\eta) - \lambda_2 \exp(-\lambda_1\eta)]$$

$$f_{r\theta}^{0(k)} = [1 + B_5^{(k)}\rho] A_3^{(k)} \exp(-\lambda_1\eta)$$

$$f_{rz}^{0(k)} = [\tfrac{1}{2}B_1^{(k)}\rho^2 + \rho + B_3^{(k)}][A_2^{(k)}\lambda_1\lambda_2] \times [\exp(-\lambda_1\lambda_2\eta) - \exp(-\lambda_1\eta)]$$

$$f_{z\theta}^{0(k)} = [\tfrac{1}{2}B_5^{(k)}\rho^2 + \rho + B_7^{(k)}] A_3^{(k)} \lambda_1 \exp(-\lambda_1\eta) \tag{17}$$

$$f_{zz}^{0(k)} = [\tfrac{1}{6}B_1^{(k)}\rho^3 + \tfrac{1}{2}\rho^2 + B_3^{(k)}\rho + B_4^{(k)}][A_2^{(k)}\lambda_1^2\lambda_2] \times [\lambda_2 \exp(-\lambda_1\lambda_2\eta) - \exp(-\lambda_1\eta)]$$

$$f_{\theta\theta}^{0(k)} = -[\bar{S}_{12}^{(k)} f_{rr}^{0(k)} + \bar{S}_{23}^{(k)} f_{zz}^{0(k)} + \bar{S}_{26}^{(k)} f_{r\theta}^{0(k)}] / \bar{S}_{22}^{(k)}$$

where $\bar{S}_{ij}^{(k)}$ are anisotropic compliances in the kth ply. In addition, according to the "strain-displacement" and "strain-stress" relationships, the circumferential stress $f_{\theta\theta}^{0(k)}$, which is dropped in the zeroth-order approximation, can be obtained by setting the boundary-layer circumferential strain $\epsilon_{\theta\theta}^{0(k)}$ to be zero.[8]

E. Complementary Energy Minimization

The total stress components can be obtained by combining the interior stress solutions and boundary-layer stress solutions as follows:

$$\begin{aligned}
\sigma_{rr}^{(k)} &= \sigma_{rr}^{0(k)} + f_{rr}^{0(k)} \\
\sigma_{\theta\theta}^{(k)} &= \sigma_{\theta\theta}^{0(k)} + f_{\theta\theta}^{0(k)} \\
\tau_{r\theta}^{(k)} &= \tau_{r\theta}^{0(k)} + f_{r\theta}^{0(k)} \\
\tau_{rz}^{(k)} &= f_{rz}^{0(k)} \\
\tau_{z\theta}^{(k)} &= f_{z\theta}^{0(k)} \\
\sigma_{zz}^{(k)} &= f_{zz}^{0(k)}
\end{aligned} \tag{18}$$

Among the total stress components, the remaining two undetermined parameters λ_1 and λ_2 are determined by the complementary energy minimization for the zeroth order. In addition, the external work has no contribution to complementary energy minimization due to its independence with respect to λ_1 and λ_2. Therefore, we can obtain

$$\begin{aligned}
\delta\Pi_c = \delta \Bigg\{ \sum_{k=1}^{N} \frac{1}{2} \int_{-\pi}^{\pi} \int_{0}^{1} \int_{0}^{\infty}_{V^{(k)}} & [(\hat{S}_{11} f_{rr}^0 + \hat{S}_{13} f_{zz}^0 + \hat{S}_{16} f_{r\theta}^0) f_{rr}^0 \\
& + (\hat{S}_{13} f_{rr}^0 + \hat{S}_{33} f_{zz}^0 + \hat{S}_{36} f_{r\theta}^0) f_{zz}^0 + (\hat{S}_{16} f_{rr}^0 + \hat{S}_{36} f_{zz}^0 \\
& + \hat{S}_{66} f_{r\theta}^0) f_{r\theta}^0 + (\hat{S}_{44} f_{z\theta}^0 + \hat{S}_{45} f_{rz}^0) f_{z\theta}^0 + (\hat{S}_{45} f_{z\theta}^0 \\
& + \hat{S}_{55} f_{rz}^0) f_{rz}^0](R + t\eta) t^2 \, d\eta \, d\rho \, d\theta \Bigg\} = 0
\end{aligned} \tag{19}$$

where

$$\hat{S}_{ij}^{(k)} = \bar{S}_{ij}^{(k)} - \bar{S}_{2i}^{(k)} \bar{S}_{2j}^{(k)} / \bar{S}_{22}^{(k)}$$

Substituting the stress expressions (17) into Eq. (19) and then taking partial derivatives with respect to λ_1 and λ_2 yield the following two nonlinear simultaneous algebraic equations:

$$\begin{aligned}
\frac{\partial \Pi_c}{\partial \lambda_1} = \{ & \lambda_1^5 R(3\lambda_2^5 P_{33} + 3\lambda_2^4 P_{33}) + \lambda_1^4 t(2\lambda_2^4 P_{33}) \\
& + \lambda_1^3 R[\lambda_2^4(-2P_{13} - 2P_{36} + P_{44} + 2P_{45} + P_{55}) \\
& + \lambda_2^3(-2P_{13} - 2P_{36} + 2P_{44} + 2P_{45} + P_{55}) + \lambda_2^2 R P_{44}] \\
& - \lambda_1 R[\lambda_2^4(P_{11} + 2P_{16} + P_{66}) + \lambda_2^3(4P_{11} + 6P_{16} + 2P_{66}) \\
& + \lambda_2^2(4P_{11} + 4P_{16} + 2P_{66}) + \lambda_2 P_{11}] \\
& - t[\lambda_2^4(P_{11} + 2P_{16} + P_{66}) + \lambda_2^3(4P_{11} + 6P_{16} + 2P_{66}) \\
& + \lambda_2^2(8P_{11} + 8P_{16} + P_{66}) + 4\lambda_2 P_{11} + P_{11}] \} = 0
\end{aligned} \tag{20}$$

$$\begin{aligned}
\frac{\partial \Pi_c}{\partial \lambda_2} = \{ & \lambda_2^6 R(\lambda_1^5 P_{33}) + \lambda_2^5(3\lambda_1^5 P_{33}) + \lambda_2^4[2\lambda_1^5 R P_{33} \\
& + 2\lambda_1^4 t P_{33} + \lambda_1^3 R(-2P_{13} - 2P_{36} + 2P_{45} + P_{55}) \\
& - \lambda_1^2 t(-2P_{13} - 3P_{36} + P_{45} + P_{55}) - \lambda_1 R(2P_{11} + 2P_{16}) \\
& - t(P_{11} + P_{16})] + \lambda_2^3[\lambda_1^3 R(-2P_{13} - 2P_{36} + 2P_{45} + P_{55}) \\
& + \lambda_1^2(-2P_{13} - P_{36} + 3P_{45} + P_{55}) - \lambda_1 R(4P_{11} + 2P_{16}) \\
& - t(6P_{11} + 5P_{16})] - \lambda_2^2(3\lambda_1 R P_{11} + 6t P_{11}) \\
& - \lambda_2(\lambda_1 R P_{11} + 4t P_{11}) - t P_{11} \} = 0
\end{aligned} \tag{21}$$

The expressions for P_{ij} are listed next and calculated by 32-point Gaussian quadrature formulas:

$$P_{11} = \sum_{k=1}^{N} \int_{-\pi}^{\pi} [\hat{S}_{11}^{(k)} p_1^2 q][1 + B_1^{(k)} + \tfrac{1}{3}B_1^{(k)^2}]\, d\theta$$

$$P_{13} = \sum_{k=1}^{N} \int_{-\pi}^{\pi} \hat{S}_{13}^{(k)} p_1^2 q[\tfrac{1}{6} + \tfrac{1}{6}B_1^{(k)} + \tfrac{1}{2}B_3^{(k)} + B_4^{(k)} + \tfrac{1}{3}B_1^{(k)}B_3^{(k)} + \tfrac{1}{2}B_1^{(k)}B_4^{(k)} + \tfrac{1}{30}B_1^{(k)^2}]\, d\theta$$

$$P_{16} = \sum_{k=1}^{N} \int_{-\pi}^{\pi} \hat{S}_{16}^{(k)} p_1 p_2 q\{1 + \tfrac{1}{3}B_1^{(k)}B_5^{(k)} + \tfrac{1}{2}[B_1^{(k)} + B_5^{(k)}]\}\, d\theta$$

$$P_{33} = \sum_{k=1}^{N} \int_{-\pi}^{\pi} \hat{S}_{33}^{(k)} p_1^2 q[1/20 + \tfrac{1}{36}B_1^{(k)} + \tfrac{1}{4}B_3^{(k)} + \tfrac{1}{3}B_4^{(k)} + \tfrac{1}{15}B_1^{(k)}B_3^{(k)} + \tfrac{1}{12}B_1^{(k)}B_4^{(k)} + B_3^{(k)}B_4^{(k)} + \tfrac{1}{252}B_1^{(k)^2} + \tfrac{1}{3}B_1^{(k)^2} + B_4^{(k)^2}]\, d\theta$$

$$P_{36} = \sum_{k=1}^{N} \int_{-\pi}^{\pi} \hat{S}_{36}^{(k)} p_1 p_2 q[\tfrac{1}{6} + \tfrac{1}{24}B_1^{(k)} + \tfrac{1}{2}B_3^{(k)} + B_4^{(k)} + \tfrac{1}{8}B_5^{(k)} + \tfrac{1}{30}B_1^{(k)}B_5^{(k)} + \tfrac{1}{3}B_3^{(k)}B_5^{(k)} + \tfrac{1}{2}B_4^{(k)}B_5^{(k)}]\, d\theta \tag{22}$$

$$P_{66} = \sum_{k=1}^{N} \int_{-\pi}^{\pi} \hat{S}_{66}^{(k)} p_2^2 q[1 + B_5^{(k)} + \tfrac{1}{3}B_5^{(k)^2}]\, d\theta$$

$$P_{44} = \sum_{k=1}^{N} \int_{-\pi}^{\pi} \hat{S}_{44}^{(k)} p_2^2 q[\tfrac{1}{3} + \tfrac{1}{4}B_5^{(k)} + B_7^{(k)} + \tfrac{1}{20}B_5^{(k)^2} + \tfrac{1}{3}B_5^{(k)}B_7^{(k)} + B_7^{(k)^2}]\, d\theta$$

$$P_{45} = \sum_{k=1}^{N} \int_{-\pi}^{\pi} \hat{S}_{45}^{(k)} p_1 p_2 q[\tfrac{1}{3} + \tfrac{1}{8}B_1^{(k)} + \tfrac{1}{2}B_3^{(k)} + \tfrac{1}{8}B_5^{(k)}\tfrac{1}{2}B_7^{(k)} + \tfrac{1}{20}B_1^{(k)}B_5^{(k)} + \tfrac{1}{6}B_1^{(k)}B_7^{(k)} + \tfrac{1}{6}B_3^{(k)}B_5^{(k)} + B_3^{(k)}B_7^{(k)}]\, d\theta$$

$$P_{55} = \sum_{k=1}^{N} \int_{-\pi}^{\pi} \hat{S}_{44}^{(k)} p_1^2 q[\tfrac{1}{3} + \tfrac{1}{4}B_1^{(k)} + B_3^{(k)} + \tfrac{1}{20}B_1^{(k)^2} + \tfrac{1}{3}B_1^{(k)}B_3^{(k)} + B_3^{(k)^2}]\, d\theta$$

where $p_1 = a_1^{(k)}$, $p_2 = a_3^{(k)}$, and $q = t_0^{(k)^2}$.

The solution procedures for solving the nonlinear simultaneous equations (20) and (21) are the same as those of Ref. 6

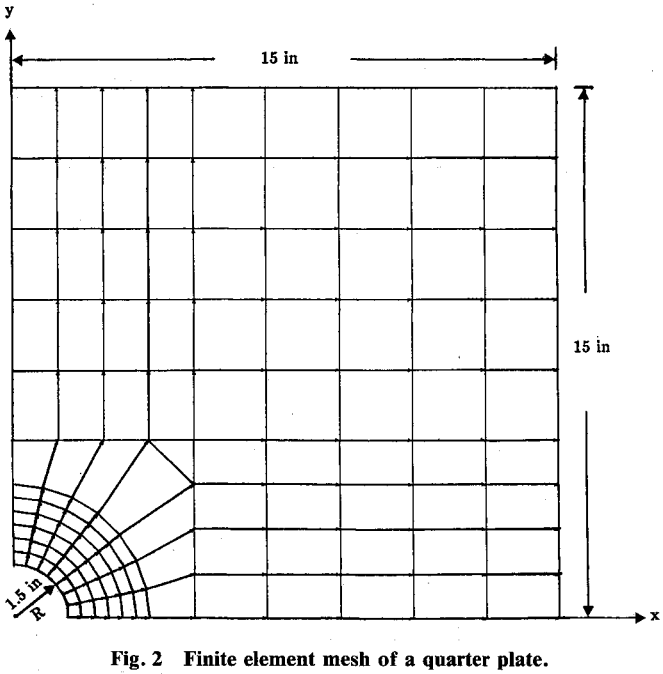

Fig. 2 Finite element mesh of a quarter plate.

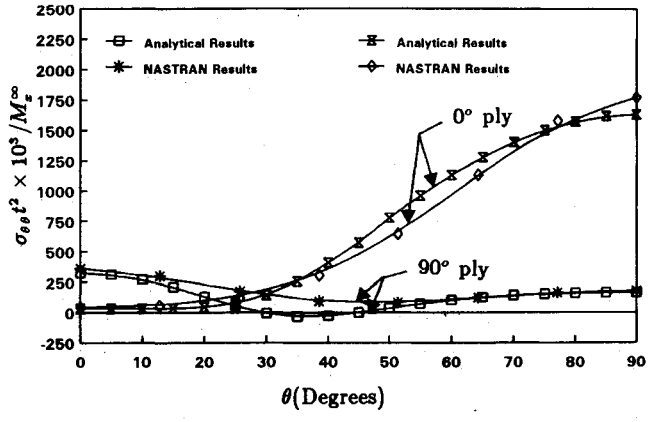

Fig. 3 Circumferential ply stress $\sigma_{\theta\theta}$ around a circular hole of a (90/0 deg)$_s$ laminate under pure bending.

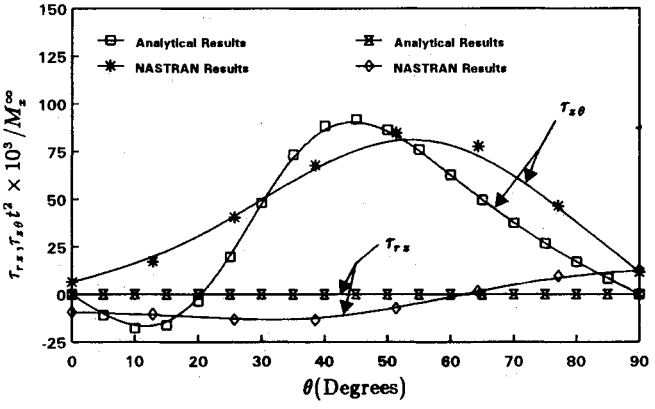

Fig. 4 Interlaminar shear stress τ_{rz} and $\tau_{z\theta}$ around a circular hole at 90/0 deg interface of a (90/0 deg)$_s$ laminate.

and are followed in the present analysis. Here, the Newton-Raphson iterative method is used, and a recommended initial value for λ_1 is 1.0 (1/in.).

III. Numerical Results and Finite Element Solutions

To check the accuracy and efficiency of the current method, numerical results obtained from the present solution are compared with those obtained by using the NASTRAN finite element computer program.[18] The problem considered herein is that of a (90/0 deg)$_s$ composite laminate subjected to uniaxial pure bending $M_x^\infty = 1$ lb-in./in. The material properties with respect to principal material axes of each ply for boron/epoxy and geometry of the laminate used in the present study are given by $E_{11} = 30.0$ Msi, $E_{22} = E_{33} = 3.0$ Msi, $G_{12} = G_{13} = G_{23} = 1.0$ Msi, $\nu_{12} = \nu_{13} = \nu_{23} = 0.336$, $R = 1.5$ in., and $t = 0.05$ in. The present problem of an infinite composite laminate with a hole is modeled by a large square plate with the outer dimensions equal to 10 times the hole diameter. This approximation will not significantly affect the stress distributions around the hole, which is the region of interest. In the finite element analysis, conventional three-dimensional solid elements based on displacement formulation are used to model each ply of the laminate. Because of the symmetry, only one quarter of the laminated plate is modeled and shown in Fig. 2. To account for the steep stress gradients around the hole, a relatively fine mesh is used. The final results given in this paper are obtained from the mesh with 460 elements and 700 nodes. Numerical results calculated from the present solution along with those of the finite element method are shown in Figs. 3–6. Figure 3 displays the circumferential stress $\sigma_{\theta\theta}$ distributions for 90 and 0 deg plies along the edge of the hole (i.e., at $r = R$) at the upper 90/0 deg interface location. It is seen that the agreement between the two sets of results is good. Figures 4 and 5 show

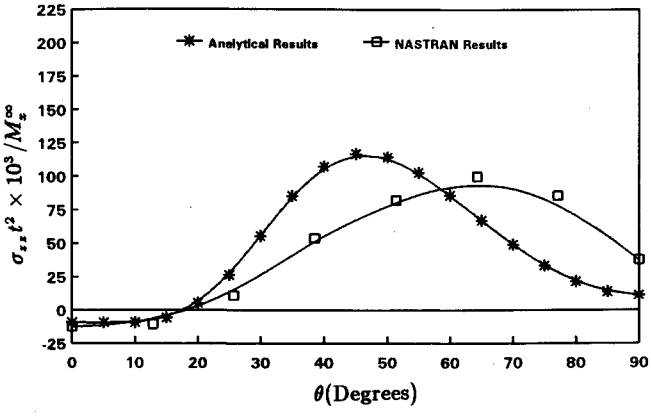

Fig. 5 Interlaminar normal stress σ_{zz} around a circular hole at 90/0 deg interface of a (90/0 deg)$_s$ laminate.

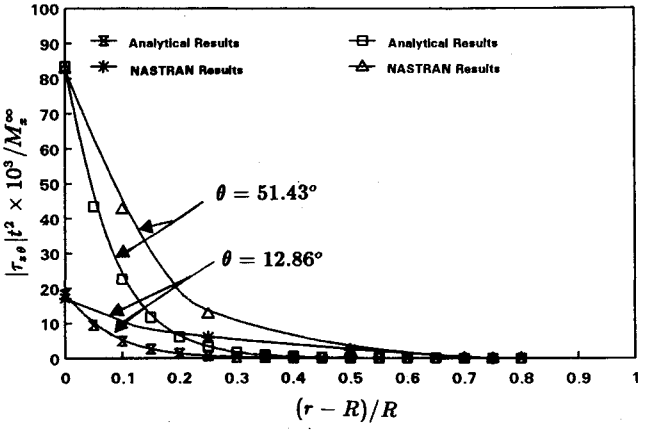

Fig. 6 Interlaminar shear stress $\tau_{z\theta}$ distributions at 90/0 deg interface of a (90/0 deg)$_s$ laminate under pure bending.

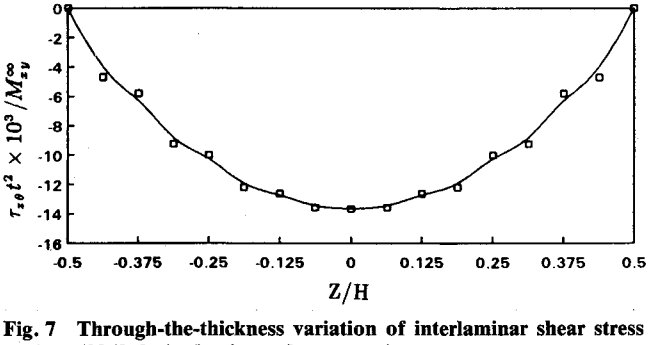

Fig. 7 Through-the-thickness variation of interlaminar shear stress $\tau_{z\theta}$ in a (90/0 deg)$_{4s}$ laminate due to torsion.

the interlaminar shear and normal stress along the hole edge of the 90/0 deg interface. It can be observed that the trends depicted by both methods are similar, and the values of peak stress agree well. As a result, the finite element method solutions qualitatively verify the current method. In view of Fig. 4, the interlaminar shear stress τ_{rz} obtained by the current solution satisfies the traction-free boundary condition at the hole edge. However, results from the finite element method do not satisfy exactly. It seems that this effect is the primary reason for the discrepancies of the interlaminar shear stress $\tau_{z\theta}$ and interlaminar normal stress σ_{zz} of both methods. In Fig. 6, comparisons of the magnitude of interlaminar shear stress $\tau_{z\theta}$ are presented at two different finite element nodal locations $\theta = 12.86$ and 51.43 deg with respect to the nondimensional radial coordinate $(r - R)/R$ at the upper 90/0 deg interface. The reason for selecting these two locations is mainly because

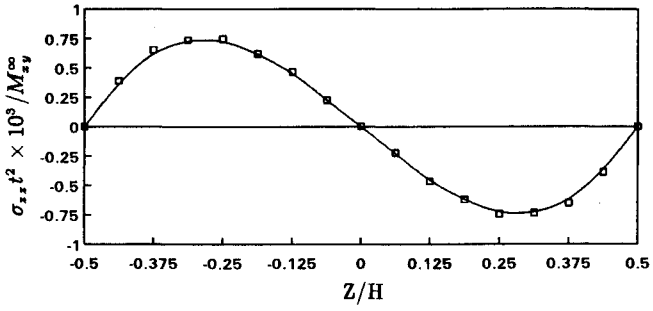

Fig. 8 Through-the-thickness variation of interlaminar normal stress σ_{zz} in a (90/0 deg)$_{4s}$ laminate due to torsion.

of the better consistency for the magnitude of the interlaminar shear stresses $\tau_{z\theta}$, as shown in Fig. 4, by the current solution and finite element method. Therefore, the attenuation of interlaminar shear stresses $\tau_{z\theta}$ obtained by both methods can be easily compared. It is seen that interlaminar shear stress $\tau_{z\theta}$ calculated from the current analytical solution attenuates more quickly than those obtained by the finite element method. For the preceding example, the current technique yields a solution in under 3 s of CPU time on the CDC 180/830 computer system whereas the NASTRAN finite element method requires 777 s of CPU time on the same computer system. In addition, owing to the antisymmetric deformation for cross-ply laminates under torsional load, a full plate model is required in the finite element analysis. Consequently, more execution time is consumed for the finite element analysis of torsional load.

The variations of interlaminar shear stress $\tau_{z\theta}$ and normal stress σ_{zz} through the thickness and at $\theta = 60$ deg of a (90/0 deg)$_{4s}$ laminate subjected to pure torsional load $M_{xy}^\infty = 1$ lb-in./in. are shown in Figs. 7 and 8. As shown, the peak value of the interlaminar shear stress $\tau_{z\theta}$ is at the midplane of the laminate. However, there is no interlaminar normal stress σ_{zz} existing at the midplane.

IV. Conclusions

An efficient analytical method to calculate all stress components around a circular hole in symmetric cross-ply laminates under a set of far-field bending and torsional loads is presented. The present solution is valid for symmetric cross-ply laminates, and it cannot account for general symmetric laminates. The main difficulty arises from the presence of the bending-torsion coupling stiffness D_{16} and D_{26}. Further investigations are needed for laminates with general symmetric constructions.

Acknowledgment

This paper is a part of the research work supported by a research grant from the National Science Council, Republic of China.

References

[1]Pipes, R. B., and Pagano, N. J., "Interlaminar Stresses in Composite Laminates under Uniform Axial Extension," *Journal of Composite Materials,* Vol. 4, Oct. 1970, pp. 538–548.

[2]Salamon, N. J., "Interlaminar Stresses in Layered Composite Laminates in Bending," *Journal of Fiber Science and Technology,* Vol. 2, 1978, pp. 305–317.

[3]Wang, A. S. D., and Crossman, F. W., "Some New Results on Edge Effect in Symmetric Composite Laminates," *Journal of Composite Materials,* Vol. 11, Jan. 1977, pp. 92–106.

[4]Chan, W. S., and Ochoa, O. O., "An Integrated Finite Element Model of Edge-Delamination Analysis for Laminates due to Tension, Bending, and Torsion Loads," *Proceedings of the AIAA/ASME/ASCE/AHS 28th Structures, Structural Dynamics and Materials Conference,* AIAA, New York, April 1987 (AIAA Paper 87-0704).

[5]Wang, S. S., and Choi, I., "Boundary-Layer Effect in Composite Laminates Part I—Free Edge Stress Singularities," *ASME Journal of Applied Mechanics,* Vol. 49, Sept. 1982, pp. 541–548.

[6]Kassapoglou, C., and Lagace, P. A., "An Efficient Method for the Calculation of Interlaminar Stresses in Composite Materials," *ASME Journal of Applied Mechanics,* Vol. 53, Dec. 1986, pp.744–750.

[7]Reiss, E. L., "Extension of an Infinite Plate with a Circular Hole," *SIAM Journal,* Vol. 14, 1963, pp. 840–854.

[8]Tang, S., "Interlaminar Stresses Around Circular Cutouts in Composite Plates Under Tension," *AIAA Journal,* Vol. 15, No. 11, 1977, pp. 1631–1637.

[9]Zhang, K. D., and Ueng, C. E. S., "A Simplified Approach for Interlaminar Stresses Around a Hole in $(0°/90°)_s$ Laminates," *Journal of Composite Materials,* Vol. 22, Feb. 1988, pp. 192–202.

[10]Rybicki, E. F., and Schmuesser, D. W., "Effect of Stacking Sequence and Lay-Up Angle on Free Edge Stresses Around a Hole in a Laminate Plate Under Tension," *Journal of Composite Materials,* Vol. 12, July 1978, pp. 300–313.

[11]Carlsson, L., "Interlaminar Stresses at a Hole in a Composite Member Subjected to In-Plane Loading," *Journal of Composite Materials,* Vol. 17, May 1983, pp. 238–249.

[12]Lucking, W. M., Hoa, S. V., and Sanker, T. S., "The Effect of Geometry on the Interlaminar Stresses of $(0°/90°)_s$ Composite Laminates with Circular Holes," *Journal of Composite Materials,* Vol. 17, March 1984, pp. 188–198.

[13]Ericson, K., Persson, M., Carlsson, L., and Gustavsson, A., "On the Prediction of the Initiation of Delamination in a $(0°/90°)_s$ Laminate with a Circular Hole," *Journal of Composite Materials,* Vol. 18, Sept. 1984, pp. 495–506.

[14]Spilker, R. L., and Chou, S. C., "Edge Effects in Symmetric Composite Laminates: Importance of Satisfying the Traction-Free-Edge Condition," *Journal of Composite Materials,* Vol. 14, Jan. 1980, pp. 2–20.

[15]Ko, C. C., and Lin, C. C., "Method for Calculating the Interlaminar Stresses in Symmetric Laminates Containing a Circular Hole," *AIAA Journal,* Vol. 30, No. 1, 1992, pp. 197–204.

[16]Bradshaw, R. D., and Pang, S. S., "Failure Analysis of Composite Laminated Plates with Circular Holes Under Bending," *The 14th Annual Energy-Sources Technology Conference and Exhibition,* sponsored by the Petroleum Division, American Society of Mechanical Engineers, New York, Vol. 37, 1991, pp. 125–135.

[17]Lekhnitskii, S. G., *Anisotropic Plates,* Gordon & Breach, New York, 1968.

[18]McCormick, C. W., *The NASTRAN User's Manual,* McNeal-Schwendler, Los Angeles, 1983.

[19]Jones, R. M., *Mechanics of Composite Materials,* McGraw-Hill, New York, 1970.